An all-silicone zoom lens in an optical imaging system*

Zhao Cun-Hua(赵存华)†

College of Physics and Electronic Information, Luoyang Normal University, Luoyang 471022, *China*
Luoyang Key Laboratory of Laser Spectrum Technology, Luoyang 471022, *China*
Institute of Modern Optics, Luoyang Normal University, Luoyang 471022, *China*

(Received 6 November 2012; revised manuscript received 16 May 2013)

An all-silicone zoom lens is fabricated. A tunable metal ringer is fettered around the side edge of the lens. A nylon rope linking a motor is tied, encircling the notch in the metal ringer. While the motor is operating, the rope can shrink or release to change the focal length of the lens. A calculation method is developed to obtain the focal length and the zoom ratio. The testing is carried out in succession. The testing values are compared with the calculated ones, and they tally with each other well. Finally, the imaging performance of the all-silicone lens is demonstrated. The all-silicone lens has potential uses in cellphone cameras, notebook cameras, micro monitor lenses, etc.

Keywords: micro lens, silicone lens, zoom, optical system

PACS: 42.79.Bh, 95.75.De **DOI:** 10.1088/1674-1056/22/9/094214

1. Introduction

Zoom lenses are widely used in industry, research fields, civilian products, and weaponry. Nevertheless, micro zoom lens cannot be realized using traditional glass/plastic materials. Adaptive lenses must be developed for they do not need to move optical elements for realizing zooming, which can economize most of the weight and bulk. So far, some adaptive micro zoom lenses have been put forward such as liquid zoom lenses,[1–4] liquid crystal zoom lenses,[5,6] or the stimuli-responsive hydro gel micro lens.[7]

In 1875, Lippmann studied the electro-capillary phenomenon.[8] In 1936, Frumkin[9] studied the electrowetting phenomenon. In 1995, Gorman *et al.*[10] first realized a liquid zoom lens by the electrowetting effect. Liquid lenses are divided into two types: the mechanical type and the electrowetting type. The mechanical liquid lens uses the changeable transparent liquid chamber to alter the curvature radius of the liquid surface to realize zoom. The mechanical liquid lens needs a motor to drive the liquid from the storage to the chamber. Several different mechanical liquid lenses were designed by various research groups.[3,11–13] They only designed, fabricated, tested, and analyzed the liquid zoom lenses using different methods. Their substantial application has not been brought into effect. The electrowetting liquid lens realizes zoom using the electrowetting effect, which consists of two similar density liquids (a conductive liquid and an insulative liquid). When a voltage is exerted between the conductive liquid and a metal electrode, the liquid surface tension will drive the liquid interface to change to realize zoom. The maximum disadvantage of the liquid lens is its sealability which may reduce its lifetime. The electrowetting liquid lens is more feasible but more complicated, thereby restricting its industrialization. A variable-focus electrowetting liquid lens for miniaturizing cameras was designed by Kuiper and Hendriks[14] in Philips Research Eindhoven. Good image quality was obtained. In order to keep the image stable, Peng *et al.*[9] investigated a zoom lens without motorized optical elements by theoretical calculation.

The liquid crystal lens realizes zoom using its anisotropy. When an electromagnetic field exists in the liquid crystal, its optical properties will change in different directions. Therefore, the refractive index of the liquid crystal varies in different directions. The liquid crystal behaves like a lens instead of a parallel plate. The different focal lengths will be obtained through changing the electromagnetic field magnitude. The liquid crystal zoom lens cannot obtain a large zoom ratio because of its particular structure. Ren and Wu[15] investigated the adaptive liquid crystal lens with large focal length tenability.

A stimuli-responsive hydrogels micro lens was reported.[7] The hydrogels need to respond to the environmental temperature or pH value. The adaptive zoom lens of the stimuli-responsive hydrogels responds very slowly, so it is very difficult to popularize it in electronic products. In addition, it is impossible for large-scale temperature variation to take place in consumer electronic products. Only one paper about using this method to realize zoom has been found.[7]

All-silicone lenses were used in intraocular corrections.[16–18] A silicone glass concentrator lens was also invented.[19] According to the literature at hand, the all-silicone zoom lens has not been found in an optical imaging system. In this paper, an all-silicone zoom lens for an optical imaging system is fabricated using elastic polydimethylsilox-

*Project supported by the Foundation of Science & Technology Department of Henan Province, China (Grant No. 102102210477) and the Foundation of Science & Technology Bureau of Luoyang City, China (Grant No. 1101040A).

†Corresponding author. E-mail: zhao.cun.hua@163.com

© 2013 Chinese Physical Society and IOP Publishing Ltd

ane (PDMS). The PDMS is Dowconing's SYLGARD® 184 PDMS that has two liquids: the silicone elastomer base and the silicone elastomer current agent. They are mixed with a ratio of 10:1 (ten is for the base and one is for the current agent). The liquid mixture concretes into a solid after air drying for some time. A thermostatic oven is sometimes used to accelerate the air drying. An all-silicone lens is formed in a metal mold. The zoom lens is assembled. Finally, its imaging performance is evaluated. Using the light transmission, elasticity and image quality as a measure of the all-silicone lens should be a good method to analyze the optical zoom microlens system.

The all-silicone zoom lens has the merits of all solid-state, easy fabrication, large zoom ratio, and convenient miniaturization. They could potentially be used in cellphone cameras, notebook cameras, monitor lenses, etc.

2. Fabrication of the all-silicone biconvex lens

A metal mold is manufactured, consisting of respective upper/under metal covers (steel 45 with Chinese standard) and a middle hoop (two canvas layers with one absorbent cotton interlayer, like the sandwich bandage in a hospital). As illustrated in Fig. 1, the curvature radii of the inner surfaces of the upper/nether metal covers are equal to the required curvature radii of the all-silicone lens. The inner surfaces of the mold have a surface roughness of Ra 0.1 μm to ensure the refractive surface quality. The middle bibulous hoop is comprised of three layer materials, where a hole that is used to inject SYLGARD 184 mixture. The three parts of the mold are conglutinated by glue water 502.

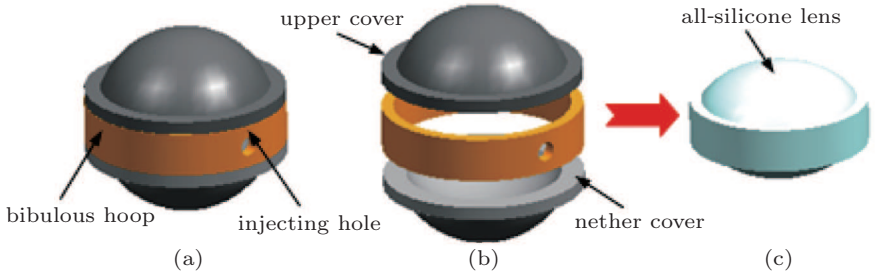


Fig. 1. (color online) Metal mold used to fabricate all-silicone lens. (a) Outline. (b) Separated parts. (c) All-silicone lens founded by the metal mold.

Our all-silicone zoom lens is fabricated using Dowconing's SYLGARD 184 PDMS that possesses good light transmission and well elasticity. The SYLGARD 184 has two parts: the silicone elastomer base and the silicone elastomer current agent. They are mixed with 10:1 ratio (10 is for base and 1 is for current agent). The mixture is injected into the metal mold via the injecting hole. Whereafter, the metal mold is placed on a bracket in a thermostatic oven with temperature of 60 °C. After one day the bibulous hoop is taken out for further dehydrating. The final all-silicone lens is obtained after two days, which is illustrated in Fig. 1(c).

The fringe bulge of the all-silicone lens as shown in Fig. 1(c) needs to be cut off. There are two main reasons for cutting off the fringe bulge: one is the abnormity after founding and the other is to eliminate the influence that results from the deformation of the lens. A tunable metal ringer is fettered around the silicone lens, leaving over a separation. A nylon rope linking a motor is tied, encircling the notch in the metal ringer. While the motor is operating, the rope can shrink or release to deform the all-silicone lens, so that its focal length is changed, as shown in Fig. 2.

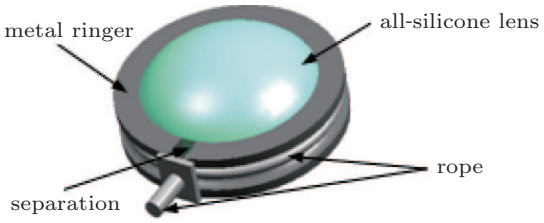


Fig. 2. (color online) Our all-silicone lens with a tunable metal ringer that has a separation and is sheaved by a rope. The rope can shrink or release to deform the silicone lens to change its focal length.

3. Approximate calculation of the all-silicone biconvex lens

Without loss of generality, supposing that the rope driven by the motor shrinks a length L. Considering Fig. 3, then a relation can be obtained as

$$\begin{aligned} &2\pi D/2 - 2\pi(D/2 - l) = L, \\ &l = L/2\pi, \end{aligned} \tag{1}$$

where D is the original aperture, and l is the half variation of the aperture. From Eq. (1), the half variation l of the aperture is in proportion to length L. The original focal length of the all-silicone lens is

$$f_0 = \frac{nR_{10}R_{20}}{(n-1)[n(R_{20} - R_{10}) + (n-1)d_0]}. \tag{2}$$

The arbitrary section plane of the all-silicone lens is shown in Fig. 3. The larger aperture lens is the original lens when the rope is in the natural state and the small aperture lens is the new lens when the rope shrinks the length L. The main parameters in Fig. 3 are illustrated in Table 1.

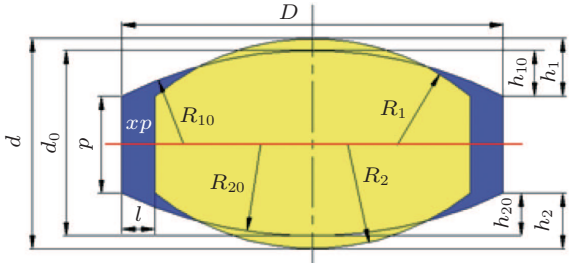


Fig. 3. (color online) Parameters of the all-silicone lens: the larger aperture lens is the original silicone lens; the small aperture lens is the new lens when its aperture changes 2l.

In Fig. 3, suppose that a plane (the horizontal solid line shown in Fig. 3) divides the silicone lens into two plano-convex lenses whose volumes are unchanged when the rope is shrinking or releasing. Thus, the volume of the upper original part lens is

$$V_{10} = \pi\left(\frac{1}{2}D\right)^2 xp + \frac{1}{3}\pi h_{10}^2(3R_{10} - h_{10}), \tag{3}$$

where x is the effective proportion taken from the whole edge for the upper lens, obviously $0 \leq x \leq 1$. When the aperture shrinks l, the volume of the upper new lens is

$$V_1 = \pi\left(\frac{1}{2}D - l\right)^2 xp + \frac{1}{3}\pi h_1^2(3R_1 - h_1), \tag{4}$$

and a simple relation from geometry can be obtained as

$$R_1 = \frac{1}{2}h_1 + \frac{(D-2l)^2}{8h_1}. \tag{5}$$

From Eqs. (3)–(5) and the condition $V_{10} = V_1$, an equation about variable sag h_1 can be obtained as

$$V = V_{10}/\pi = \left(\frac{1}{2}D - l\right)^2 xp + \frac{1}{3}h_1^2\left\{3\left[\frac{1}{2}h_1 + \frac{(D-2l)^2}{8h_1}\right] - h_1\right\}. \tag{6}$$

Equation (6) has three solutions: a real solution and two imaginary solutions. Neglecting two imaginary solutions, the sag h_1 is

$$h_1 = \frac{6D^2 - 24Dl + 24l^2}{\sqrt[3]{3844}\sqrt[3]{12D^2xp - 48Dlxp + 48l^2xp + \sqrt{4(D^2 - 4Dl + 4l^2)^3 + (12D^2xp - 48Dlxp + 48l^2xp - 48V)^2} - 48V}} - \frac{1}{2\sqrt[3]{2}}\sqrt[3]{12D^2xp - 48Dlxp + 48l^2xp + \sqrt{4(D^2 - 4Dl + 4l^2)^3 + (12D^2xp - 48Dlxp + 48l^2xp - 48V)^2} - 48V}. \tag{7}$$

Substituting Eq. (7) into Eq. (5), R_1 can be achieved. Using a similar method, the sag h_2 and the curvature radius R_2 of the nether part lens can be obtained. So far, two surface curvature radii of the new lens (the small aperture lens) are R_1 and R_2, and its central thickness is $d = h_1 + p + h_2$. The focal length of the new lens is

$$f = \frac{nR_1R_2}{(n-1)[n(R_2 - R_1) + (n-1)d]}. \tag{8}$$

For the original lens, the parameters D, n, p, d_0, R_{10}, R_{20}, h_{10}, h_{20}, and f_0 are known. In fact, in Eq. (8), there are two variables x and l. When x is given, V_{10} can be calculated by Eq. (3). Then, in Eq. (6), only variables l and h_1 exist, so variable h_1 can be solved as a function of l and R_1 is also a function of l. Finally, the focal length f in Eq. (8) of the new lens can be obtained. However, we do not know x. For solving the x, in Eq. (8), we let $l = 0$ so that the focal length f we obtained must be equal to the original focal length f_0 via Eq. (2). From this relation, we can obtain the accurate x.

The zoom ratio of the all-silicone lens is defined as the ratio of the original focal length to the new focal length. The capital M denotes the zoom ratio

$$M = \frac{f_0}{f}. \tag{9}$$

Table 1. Parameters of the all-silicone lens.

Parameter	Explanation
D	Aperture of the original lens
p	edge thickness
R_1	upper radius of the new lens
R_2	nether radius of the new lens
h_1	upper sag of the new lens
h_2	nether sag of the new lens
l	half variation of the aperture
f_0	focal length of the original lens
n	refractive index, 1.430
M	Zoom ratio
x	proportion that should be divided from whole edge for the upper lens
d	thickness of the new lens
d_0	thickness of the original lens
R_{10}	upper radius of the original lens
R_{20}	nether radius of the original lens
h_{10}	upper sag of the original lens
h_{20}	nether sag of the original lens
L	variational length of the rope
f	focal length of the new lens
V_{10}	bulk of the upper original lens
V_1	bulk of the upper new lens

4. A factual example

An actual biconvex all-silicone lens is fabricated, as shown in Section 2. Its parameters are given as follows: the radius of the upper surface $R_{10} = 25$, the radius of the nether surface $R_{20} = -20$, thickness $d_0 = 5$, refractive index $n = 1.43$, $p = 3.86$, $h_{10} = 0.502$, $h_{20} = 0.633$, $D = 10$, and $f_0 = 26.733$. The calculation process as shown in Section 3 is carried out via mathematic software. The computed results are called theoretical values including the focal lengths and the zoom ratios.

The testing configuration is set up as shown in Fig. 4. The rays emitting from a light source is picked up by an iris, so a point light source is formed. The point light source is just placed at the focus point of a collimating lens. The parallel beam from the collimating lens shots into the tested lens, namely, the all-silicone lens. The parallel beam focused at a point that should be the focus point of the tested lens. The light spot is captured by a CCD camera that is connected with a computer. All the parts were placed on a guide line. The focal length of the all-silicone lens is the distance between the silicone lens and the light spot.[20]

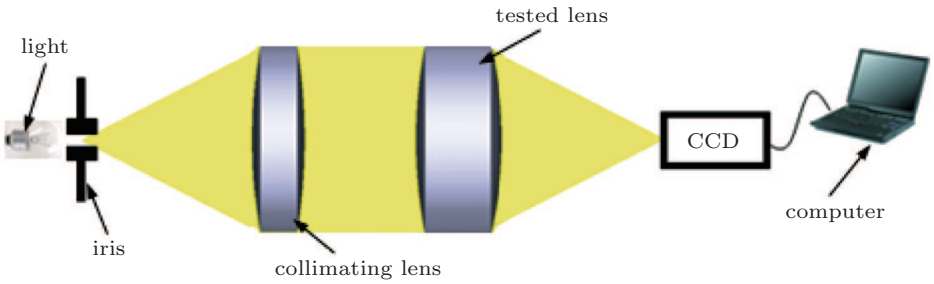


Fig. 4. (color online) Testing configuration to obtain the focal length of the all-silicone lens.

The calculated and tested results are shown in Fig. 5. The bottom x coordinate is for the shrinking length L of the rope and the top x coordinate is for the half variation of the aperture, l, determined by Eq. (1). The left y coordinate is for the focal length f of the all-silicone lens and the right y coordinate is for the zoom ratio M of the all-silicone lens. The solid curve represents the theoretical values of the focal lengths and the dash curve denotes the zoom ratio. The scattered points represent the tested values of the focal lengths (squares) and the zoom ratios (triangles).

From Fig. 5, the tested focal lengths tally well with the theoretical focal length, though a little larger than them, especially for the case of longer L or l. The theoretical and the tested results also testify the feasibility of the all-silicone lens to be used in optical zoom system.

The zoom ratio obtained from Eq. (9) is the ratio of the original focal length (long focal length) to the new focal length (short focal length). In Fig. 5, the dash curve represents the theoretical values of zoom ratio (the original focal length to the theoretical focal length) and the triangles are for the values of tested zoom ratio (the original focal length to the tested focal length). From Fig. 5, the tested values agree well with the theoretical values when $L \leq 2.5$ mm (or $l \leq 0.4$ mm), but more different when $L > 2.5$ mm (or $l > 0.4$ mm). The tested values are less than the theoretical values.

The imaging performance is shown in Fig. 6. Figure 6(a) shows a map image formed by the original lens (long focal length) and Fig. 6(b) displays the map image formed by the new lens (short focal length) with about zoom ratio $M = 2$ (the rope shrinks about 2.5 mm). From Fig. 6(b), under the short focal length, the distortion is somewhat large, especially in the fringe region. It is impossible for a single lens to correct distortion. It should be mentioned that the long shrinking length L (> 2.0 mm) will deform the silicone lens. The all-silicone lens will image asymmetrically as shown in Fig. 6(b). From Fig. 6(b), in the left bottom corner, the distortion is larger than

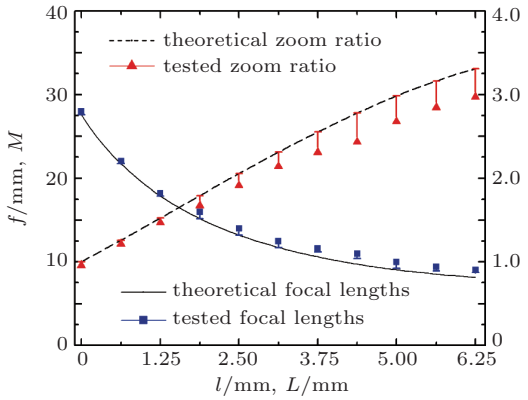


Fig. 5. (color online) Comparison between the theoretical and the tested values of the all-silicone lens. The solid curve represents the theoretical focal length; the squares represent the tested focal lengths. The dash curve shows the theoretical zoom ratio; the triangles denote the tested zoom ratios.

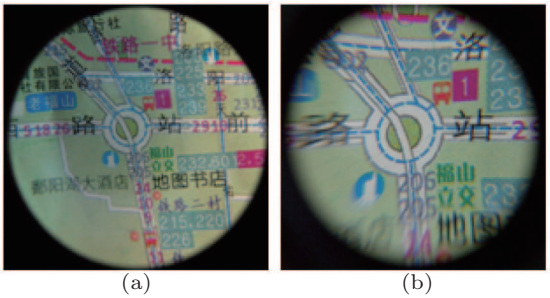


Fig. 6. (color online) Imaging performance of the all-silicone lens fabricated by us. (a) A captured map image formed by the original lens; (b) the captured map image formed by the new lens with about zoom ratio $M = 2$.

in the other fringe region. The reason for the asymmetric image is the non-homogenous pressure of the metal ringer with respect to the lens. To overcome the problem, it is necessary to seek the assistance of skilled mechanical design engineers. In fact, figure 6 does not conflict with Fig. 5. In Fig. 5, the focal lengths and the zoom ratios are calculated using the paraxial rays (to capture the minimum light point by CCD). The distortion is just the off-axial aberration, so the tested focal lengths are nothing to do with the distortion.

In brief, the all-silicone zoom lenses have potential uses in microlens-like mobile cameras, notebook cameras, monitor cameras, etc.

5. Conclusion

A metal mold is fabricated. The Dowconing SYLGARD 184 PDMS mixture is injected into the metal mold. An all-silicone lens is obtained after the PDMS mixture has air dried. An approximate model is put forward to compute the focal length for the lens. The tested focal lengths are compared with the calculated values, showing they agree well with each other. The feasibility of the all-silicone lens for optical imaging system is discussed in detail. From the viewpoint of the imaging performance, the all-silicone lens has potential uses in optical zoom microsystems.

References

[1] Kuiper S and Hendriks B 2004 *Appl. Phys. Lett.* **85** 1128
[2] Xu S, Liu Y F, Ren H W and Wu S T 2010 *Opt. Express* **18** 12430
[3] Ren H W, Fox D, Anderson P A, Wu B and Wu S T 2006 *Opt. Express* **14** 8031
[4] Zhao C H, Lu G Q, Wei D L, Hong X H, Cui D Q and Gao C L 2011 *Proc. SPIE* **8191** 81911
[5] Pouria V, David L M, Mohammad R D, Jim S, Gholam P and Peyghambarian N 2010 *Opt. Lett.* **35** 336
[6] Pouria V, Mohammad R D, Jim S, Gholam P and Peyghambarian N 2010 *Opt. Lett.* **35** 2582
[7] Liang D, Abhishek K A and David J B 2006 *Nature* **442** 551
[8] Lippmann M G 1875 *Ann. Chim. Phys.* **5** 494
[9] Frumkin A 1936 *Actual. Sci. Ind.* **373** 5
[10] Gorman B, Biebuyck H and Whitesides G 1995 *Langmuir* **11** 2242
[11] Peng R L, Chen J B, Zhu C and Zhuang S L 2007 *Opt. Express* **15** 6664
[12] Cheng H C, Xu S, Liu Y F, Levi S and Wu S T 2011 *Opt. Commun.* **284** 2118
[13] Ren H W and Wu S T 2005 *Appl. Phys. Lett.* **86** 211107
[14] Kuiper S and Hendriks H W 2004 *Appl. Phys. Lett.* **85** 1128
[15] Ren H W and Wu S T 2006 *Opt. Express* **14** 11292
[16] Pavlovic S, Jacobi F K, Graef M and Jacobi K W 2000 *J. Cataract. Refr. Surg.* **26** 88
[17] Damiana Z, Norbert S, Bernd K and Martin W 2000 *J. Cataract. Refr. Surg.* **26** 301
[18] Gholam A P and Jeffery K (U.S. patent) 5 697 973 [1997-11-16]
[19] Shin H Y, Shyu Y M, Chen C Y, Kuo H Z and Huang Y Y (U.S. patent) 8 128 852 B2 [2012-03-06]
[20] Zheng G X, Zhang R Y, Li S, He P A and Zhou H 2011 *Chin. Phys. B* **20** 117802